Electric Field in Polymeric Isolators of the 500kV Voltage Class

**Huederson Aparecido Botura Da Silva, Vitor Chaves De Oliveira,
Alexandre De Assis Mota and Lia Toledo Moreira Mota**

Department of CEATEC, Faculty of Electrical Engineering,
University of Pontifical Catholic, Campinas-Sao Paulo, CEP 13086-900, Brazil

ABSTRACT

This study presents a detailed study of the electric field in polymeric isolators of the 500kV voltage class through modifications in the dimensions of the anti-corona ring. That is, by varying the three dimensions of the anti-corona ring: height (h), distance of the anti-corona ring conductor (r) and the diameter of the anti-corona ring conductor (d); it was possible to observe the electric field distribution in a polymeric isolator of the 500 kV voltage class. Such voltage class in currently applied to prevent loss of energy in long transmission lines. However it faces disadvantages, like the problem of the increased corona effect, which besides generating electromagnetic noise, increases the level of the electric field around the conductors and the isolator. The corona effect is responsible for an electric energy loss that is in the order of hundreds of kW/km in TLs and generates noises that reach up to 65dBm. This effect occurs when the air's critical value is exceeded, causing the electrons to collide with air resulting in the formation of ozone which is a major cause of corrosion in isolators. In this study, this issue is addressed and it is outlined sizing measures for manufactoring the anti-corona ring.

Keywords: Electric Field, Transmission Line, Polymeric Isolator, Corona Effect, Anti-Corona Ring, Finite Element Method

1. INTRODUCTION

In recent years, Brazil has experienced a growth in its economy, this process has driven the expansion of various sectors, such as: commercial, residential and industrial. These three sectors have contributed in the growth of electricity consumption in Brazil, which for the last 10 years had an average growth of 4.29%, closing the year 2011 with 430,106 GWh consumed (ERC, 2012a). There is a study by the Energy Research Company (ERC) providing, in Brazil, an average growth of 4.5% in electricity consumption over the next decade (ERC, 2012b).

With the increased consumption of electricity came the need to build new electricity generating plants and as a highlight of this action, in recent years several plants started to be developed, such as: The hydroelectric of Belo Monte, with an installed capacity of 11.233 MW, Teles Pires, with an installed capacity of 1,820 MW and hydroelectric plant of Sao Luiz do Tapajós, with an installed capacity of around 7,000 MW.

The Decennial Plan of ERC predicts a growth in the Nacional Electric Interconnected System (NEIS) from 110 GW (data from December 2010) to 171 GW (forecast for December 2020) with prioritization to renewable energy sources (hydraulic, wind and biomass) (ERC, 2012c). The electricity generating power plants are usually distant from the consumer market being interconnected through Transmission Lines (TL). The growth of TL's for the decade starting from 2011 to 2020 is expected to be at 42%, making the TLs extension expand from the current 110,000 km (data from 2010)

Corresponding Author: Vitor Chaves De Oliveira, Department of CEATEC, Electrical Engineering Faculty,
Pontifical Catholic University of Campinas-São Paulo, CEP 13086-900, Brazil

rise to about 171,000 km. Among this growth it is possible to mention several other projects underway and under study, e.g., the interconnection of the Plants in the Rio Madeira, Belo Monte, Teles Pires, Tapajós, Boa Vista (Manaus) and the Interconnection Brazil-Peru (Jardini *et al*., 2011).

In these TL's the voltage class which possesses a higher growth trend is the 500 kV class, followed by the 600 kV class, with a predicted growth of 21,650 km and 14,024 km respectively. The use of extra high tension in the TLs has it's principle in the fact that the conduits are not an ideal conductor, thus there is a voltage drop resulting from passage of electric current through these conductors. This effect is known as power dissipation (Joule effect) and follows the equation: R.I², thus the lower the current that circulates through the conductors, the lower is the power dissipated.

Decreasing the current flowing through the conductors it is also possible to save on wire gauge (diameter) which, at first, directly reduces the cost of the project, as well as requesting less effort from supporting structures causing them to have a reduced cost as well.

There is also the advantage of a lower voltage drop, which emerges from Ohm's first law (V = R.I) and lower vibration, however the extra high voltage transmission not only presents advantages, it also has disadvantages such as the issue of isolation.

In electrical circuits of alternating current, the higher the voltage, the greater the possibility of a short circuit between the phases because the conductors are too close to the threshold of the dielectric rigidity of air, besides the isolation between the phases, it's also noteworthy that the isolation to the ground for these voltage levels require a more detailed attention.

Another point that can be mentioned as a disadvantage is the increased corona effect, which besides generating electromagnetic noise, increases the level of the electric field around the conductors and the isolator. Studies show that the higher the electrical potential in a TL is, the larger is the corona effect generated (Leao, 2008).

The isolator is a widely used equipment in the TLs and has in its design mechanical and electrical features. As an example of a mechanical feature it is interesting to cite the isolator's need to support mechanical efforts between its terminals, due to the conductors weight and the conduits effort with the action of the wind.

As for the electrical characteristics of the isolators it's imperative to mention their arc distance and ullage. The arc distance is essential in preventing the insolator to present failure (flashover) through disruptive discharges from lightning or closing sectionalizers switches, while the flow distance has the objective of increasing the phase potential path to the ground potential, causing the electrons in the electric current to have a longer way to travel between these two points. This flow distance is very important when climatic factors involved, such as wet weather, rain and classification of the pollution level.

In the isolators the corona effect is also present, especially in their phase terminal, this effect is shaped like a lighted crown mainly on points with abrupt changes in the shape of its surface. The corona effect is responsible for an electric energy loss that is in the order of hundreds of kW/km in TLs and generates noises that reach 65d Bm. This effect occurs when the air's critical value is exceeded (3 kV/mm) (Mello, 2007), when it happens the electrons collide with air resulting in the formation of ozone which is a major cause of corrosion in isolators, in its ironmongery or in its fiberglass core when these are used in polymeric isolators.

The polymeric isolators are being increasingly used due to its hydrophobicity characteristic being far superior to glass and porcelain materials, which are also used in manufacturing isolators. Besides this, it also reduces the number of isolators damaged by vandalism. With the use of polymeric isolators in the TLs it is possible to reduce the costs of design, which can use more compact towers by their weight reduction in comparison to glass and/or porcelain isolators. Furthermore, it's also possible to realize the project of a 800 kV TL, with the distances of a 500 kV TL used in isolators made of glass and/or porcelain. To minimize corona effect on isolators is used a device called anti-corona ring, this accessory has the purpose of equalizing the electromagnetic field and can be constructed using any conductive material, such as iron or aluminum and it may have various shapes and dimensions. The most common format is that of a circular tube.

The purpose of this study is to study the electric field distribution in a polymeric isolator of the 500 kV voltage class, by modifications in the dimensions of the anti-corona ring.

2. MATERIALS AND METHODS

2.1. Maxwell Equations

James Clerk Maxwell in 1865, presented four equations describing electromagnetic phenomena (electric and magnetic) which originated approximately 20 equations. These equations became known as the four Maxwell equations that describe the behavior of electric and magnetic fields and their interactions with matter

(substance) (Halliday *et al.*, 2010). The four Maxwell's equations are also known as.

Gauss' law of electricity (or electrostatic) expresses the relationship between the charge density and electric field. Equation (1) and (2) represent respectively differential and integral form of this law:

$$\nabla.E = \frac{\rho}{S_0} \tag{1}$$

$$\iint_{\partial v} E.dA = \frac{Q(V)}{S_0} \tag{2}$$

Gauss's magnetism Law expresses the absence of monopole in the magnetic field. Equation (3) and (4) respectively represent its differential and integral form:

$$\nabla.B = 0 \tag{3}$$

$$\iint_{\partial v} B.dA = 0 \tag{4}$$

In the Law of Induction, Faraday expressed the varying magnetic field. Equation (5) and (6) respectively represent its differential and integral form:

$$\nabla x E = -\frac{\partial B}{\partial t} \tag{5}$$

$$\int_{\partial S} E.dI = -\frac{\partial \varphi B, S}{\partial t} \tag{6}$$

Ampere's Law expresses the magnetic field source. Equation (7) and (8) respectively represent its differential and integral form, with their corrections:

$$\nabla x B = \mu 0 J + \mu_0 \varepsilon_0 \frac{\partial E}{\partial t} \tag{7}$$

$$\int_{\partial S} B.dI = \mu 0 Is + \mu_0 \varepsilon_0 \frac{\partial \varphi E, S}{\partial t} \tag{8}$$

Based on these equations it is possible to verify that electric fields generated by electrical charges that can be divergent or convergent and that magnetic fields are rotational. The magnetic fields when time varying generates electric fields, whereas the electric field when time varying generates rotational magnetic field. It is important to note that electric currents or charges in motion also generate magnetic fields.

2.2. Finite Element Method (FEM)

As established, the Maxwell's equations describe electromagnetic phenomena, however when the analysis is conducted for complex geometries, its solution becomes complex and impractical to be performed manually (Cardoso, 1995).

One of the options found to solve these problems is the use of numerical calculations. With it, it is possible to obtain an approximate solution for the problem studied and among the various existing methods of numerical calculations, the one which stands out the most for the solution of these problems is the FEM (Silva, 2012a).

In the 80's the development of processors coupled with a reduction of computer's prices in Brazil and so the FEM became popular. Since then, this method has been widely used in the academic, scientific and industrial sectors, especially for solving problems involving the distribution of electromagnetic fields in electrical equipment and systems (Cardoso, 1995).

The basic principle of the FEM is to divide the surface under study into several parts. When using two dimensions (two-dimensional) these surfaces normally have the geometry of a triangle. These small parts (triangles) are called finite elements and the set of these elements is called a mesh. The vertices of these triangles are called nodes of the mesh and it is in them that the equations to solve problems are applied (Silva, 2012a), as shown in **Fig. 1 and 2**.

2.3. Electrostatics

The electrostatic is governed by the fourth Maxwell equation, known as Gauss's Law. Equation (9) can be rewritten as equation (Silva, 2012a; Cardoso, 1995):

$$\int_S D.dS = Qi \tag{9}$$

Where:
D = Displacement Vector [C/m3].
Qi = Total amount of electrical charges involved by the closed surface

From this equation and performing the formulations described in (Cardoso, 1995; Silva, 2012a) it is possible to write the two electric field components according to Equation (10) and (11) in which the potential function inside the finite element is practically a constant:

$$E_x = -\frac{\partial V}{\partial x} = -\left(\frac{1}{2V}\right) \times (b_1 V_1 + b_2 V_2 + b_3 V_3) \tag{10}$$
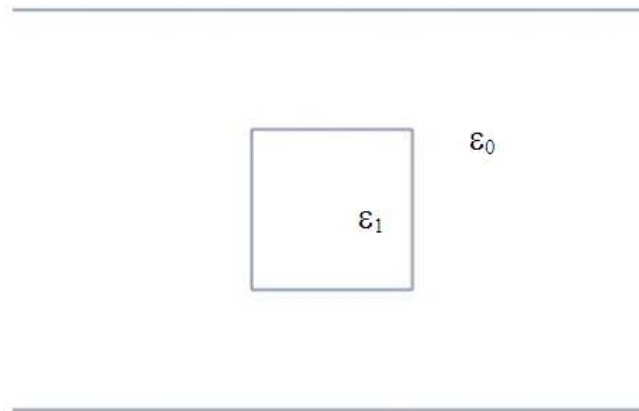
Fig. 1. Domain of study
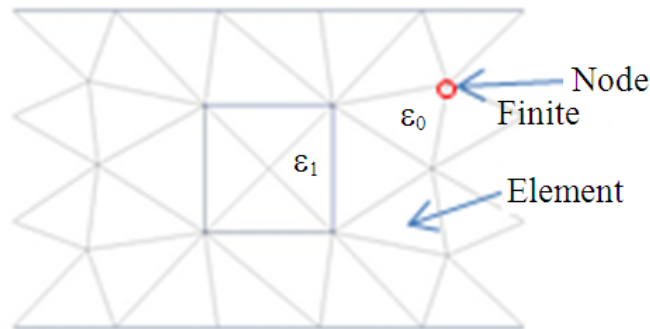
Fig. 2. Discretized domain

$$E_y = -\frac{\partial V}{\partial y} = -\left(\frac{1}{2\Delta}\right) \times (C_1 V_1 + c_2 V_2 + c_3 V_3) \qquad (11)$$

For greater accuracy in the system's resolution it is necessary to use a large amount of finite elements, however the larger the number of finite elements, the more complex is the system's resolution.

As an informative example, in a two dimensional mesh of a distributed system using three triangles, the resolution of the system will generate a 5×5 matrix, so the more components the greater the resolution array, hence the mathematics involved starts to become complex and best resolution for the system becomes the use of computational resources with specific programs to address these problems.

2.4. Use of Computer Programs

Currently, there are several computer programs applied in solving problems using the FEM, regardless of the program, it must have the same three stages, namely: pre-processing, processing and post-processing.

In the pre-processing stage it is performed: the geometry's design of the object under study, meshing (mesh generation) and imposition of physical properties of the means. As for the processing step, it is performed the assembly of the equations system and its resolution and for the post-processing stage, it is presented the magnitudes of the phenomena studied, these are represented by the field letters. This project implemented the programs Gmsh and Getdp. The program Gmsh was used in the preprocessing step, performing the design of a 500 kV voltage class isolator, generating the meshes and imposing the physical properties of the means, while the Getdp program was used in the processing and post-processing steps.

2.5. Effects of the Electric Field in the Polymeric Isolator

The electric field is a physical phenomenon and as previously defined (Halliday *et al.*, 2010), it is a vector field that consists in a distribution of vectors.
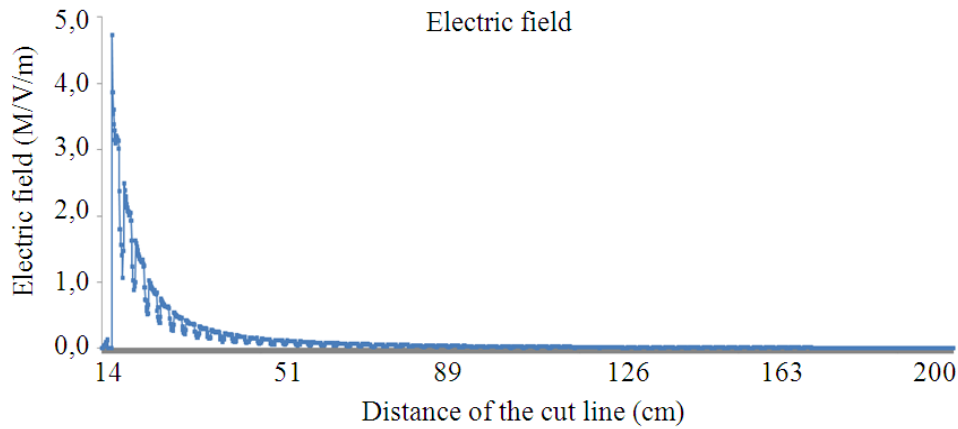
Fig. 3. Electric field intensity in the 500 kV class polymeric isolator, without the anti-corona ring

According to (Silva, 2012a) the intensity of the electric field in the 500 kV class polymeric isolator and without the anti-corona ring as displayed in the following graph in **Fig. 3**.

It is possible to observe that in the electric field intensity is shown a large peak near the phase terminal and it tends to drop over the isolator due to its dielectric properties. By inserting an anti-corona ring it is possible to observe that the initial peak of the electric field intensity decays, however there is a formation of a peak value of electric field intensity. The graph of the electric field intensity of a 500 kV class isolator can be seen in **Fig. 4**.

2.6. Methodology

This study will carry out a study of the electric field variation in a polymeric isolator of a 500 kV voltage class, manufactured by Balestro Electromechanical Industry Ltd., the model of the isolator used in this study is the IPB 500/CB/120/EAP/117, which contains an arc distance of 3065 mm and flow (flight) distance of 13,700 mm. This isolator possesses axial symmetric geometry, making it possible to design it in two dimensions and at the time for processing the system resolution the Getdp program performs the field lines simulation in a radius 2π symmetry (Silva, 2012b).

In this study it will not be considered the transmission tower structure, the type of TLs cable arrangement, nor a possible Difference in Potential (DDP) at the isolator's ground terminal due to its impedance and height of transmission tower structure. The system is solved using the "EleSta_v" library which at the simulation's moment uses the maximum voltage applied in the phase terminal and in the anti-corona ring, thus obtaining the maximum electric field intensity. The electric field is measured in the cutline of the interface silicone/air of the isolator according to **Fig. 5**.

The physical properties used in this study were: 1020 carbon steel, fiberglass, silicone, aluminum and air (Silva, 2012a) as presented in **Fig. 6**.

The simulations performed variations of the anti-corona ring physical dimensions. For a better understanding throughout this study it will be considered "d" as the diameter of the anti-corona ring conductor, "h" the height of the anti-corona ring and "r" as the distance from the center of the anti-corona ring conductor into the isolator's center core **Fig. 7**.

For each simulation performed only one of the three dimensions studied is varied. After studying one dimension, the next dimension will be analyzed and so on, until all three are studied. Initially a variation of the dimension "r" will be the performed keeping constant "h" and "d". Then the variation of "h" and then the variation of "d".

The dimensions range of this study is:

- For the dimension "d" variance begins at 1.0 cm and reaches up to 41.0 cm with a 2.0 cm variation for each simulation
- The dimension "r" varies 0.5 cm for each simulation, starting at the point in which the outer diameter stays closer to the isolator's vane until a distance of 75 cm from the conductor's center of the anti-corona ring to the isolator's core
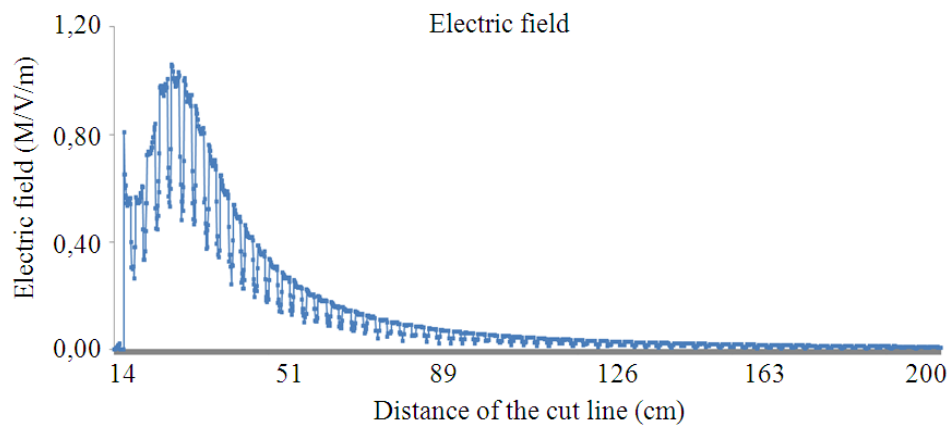
Fig. 4. Electric field intensity in the 500 kV voltage class polymeric isolator with an anti-corona ring
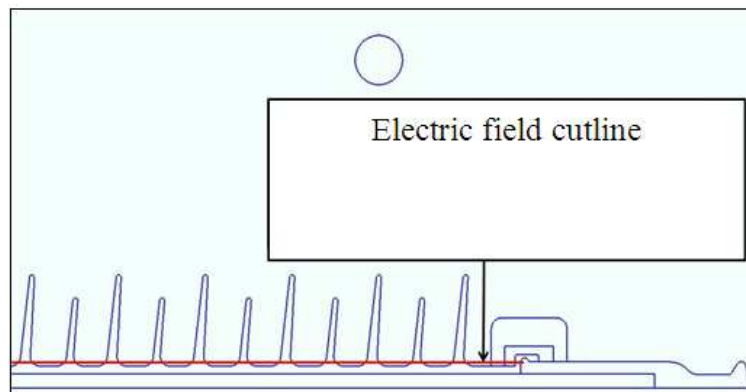
Fig. 5. Electric field cutline (Silva, 2012a)
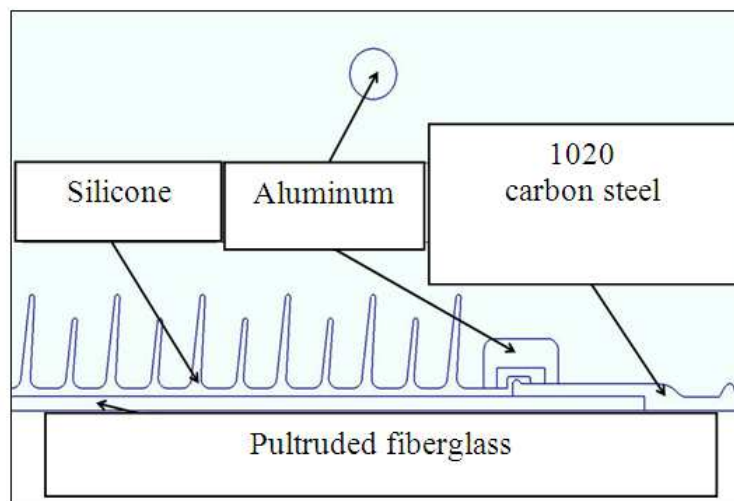
Fig. 6. Isolator's physical properties
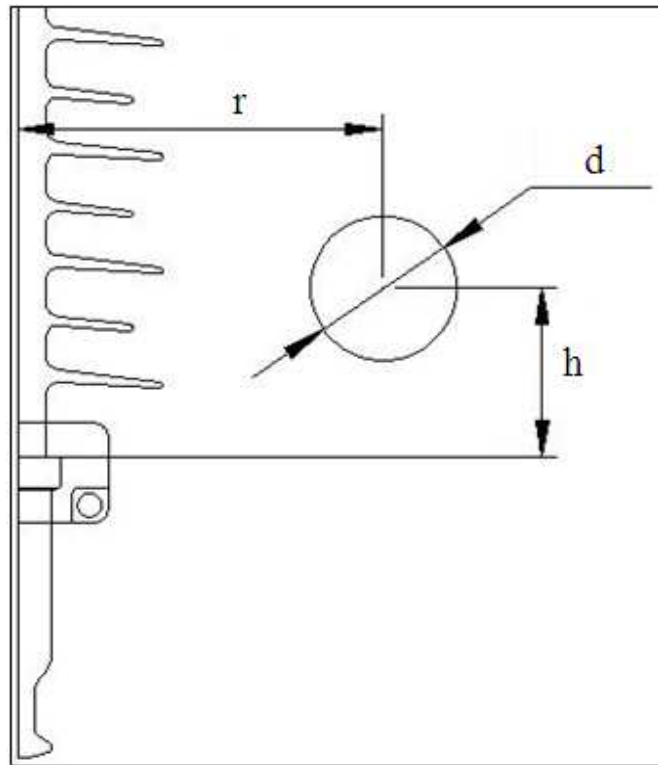
Fig. 7. Drawing showing the dimensions studied
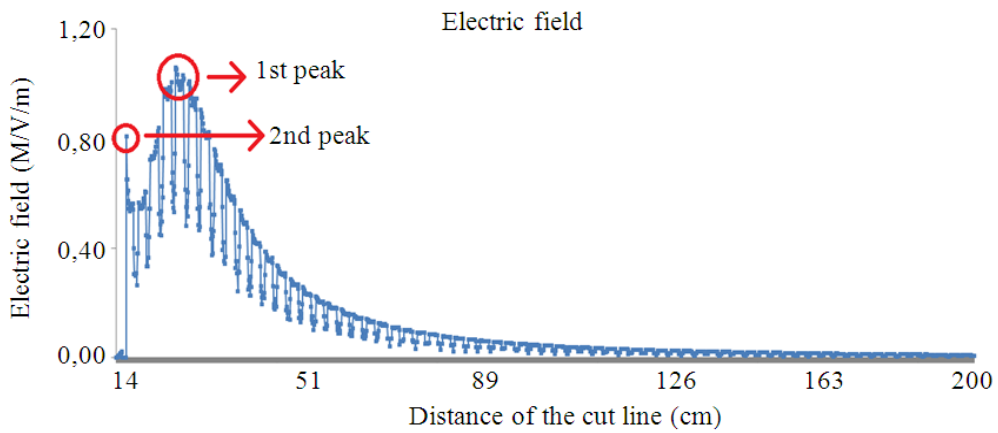
Fig. 8. Drawing showing the 1st and 2nd peaks of the electric field intensity

- Dimension "h" variance starts at 3.0 cm and reaches up to 20.0 cm with a 1.0 cm variation for each simulation

It is possible to observe that the electric field distribution presents two peaks, one peak for the isolator's phase terminal and another referring to the presence of the anti-corona ring, which will be called, respectively, 1st and 2nd peak, as shown in **Fig. 8**.

In this study it will be accepted as the minimum value for the electric field intensity a measure when the 1st peak and 2nd peaks present the same value.

3. RESULTS

With the use Gmsh and Getdp programs it was possible to obtain the field letter (chart) of the electric field and the electric field intensity graphic in the cutline under analysis. **Figure 9** shows the field letter (chart) of the electric field while **Fig. 10** shows the electric field intensity graphic for both. The simulation was performed with d = 9.0 cm, h = 6.0 cm and r = 13.0 cm.

For each simulation performed it was noted the value of the 1st and 2nd electric field peaks, making it possible to obtain the graphic in which there is an intersection of these values for a given simulations sequence. This intersection will be considered as the optimal electric field for this simulations sequence. The sequence of simulations used is the variation of "r", keeping fixed the values of "d" and "h". The graphic in **Fig. 11** shows the simulations sequence with d = 9.0 cm and h = 6.0 cm.
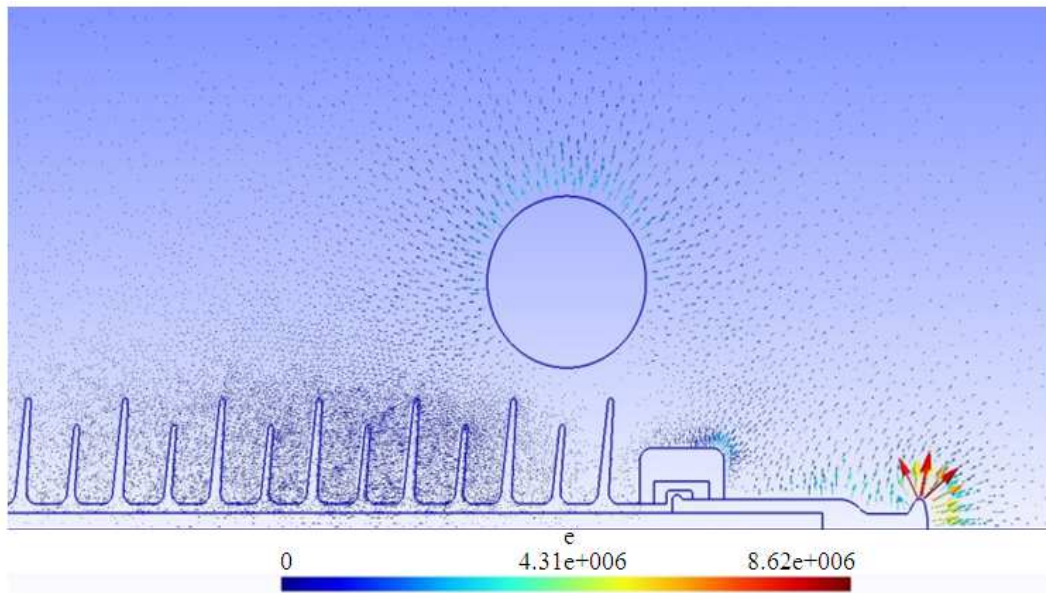
Fig. 9. Field letter (chart) of the electric field
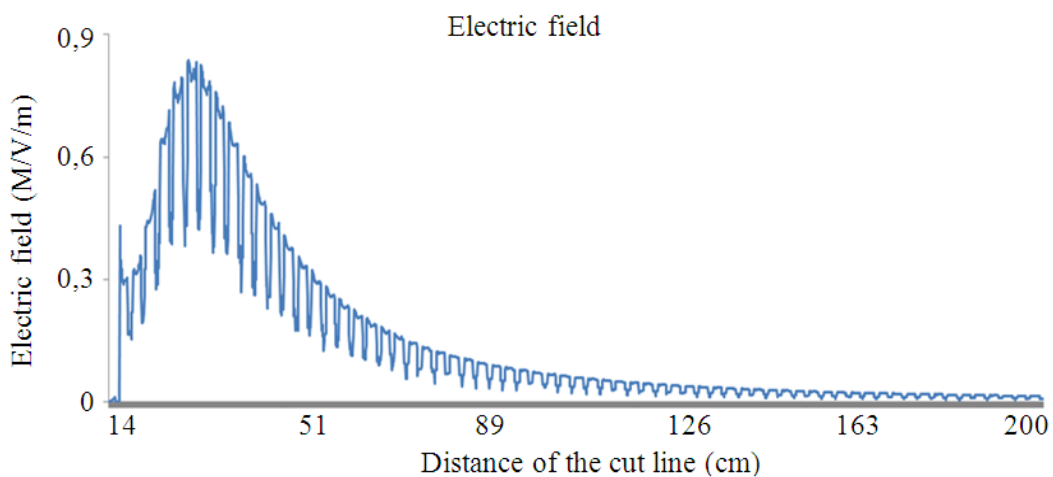
Fig. 10. Electric field graphic in the cutline
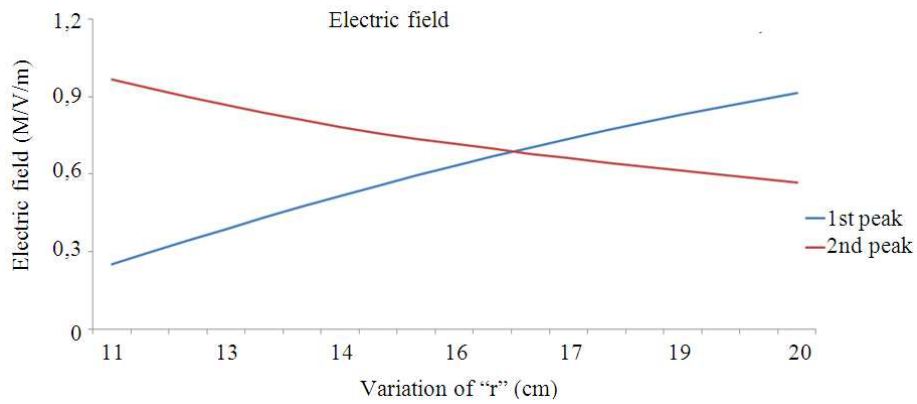
Fig. 11. Graphic showing the intersection of 1st and 2nd peaks
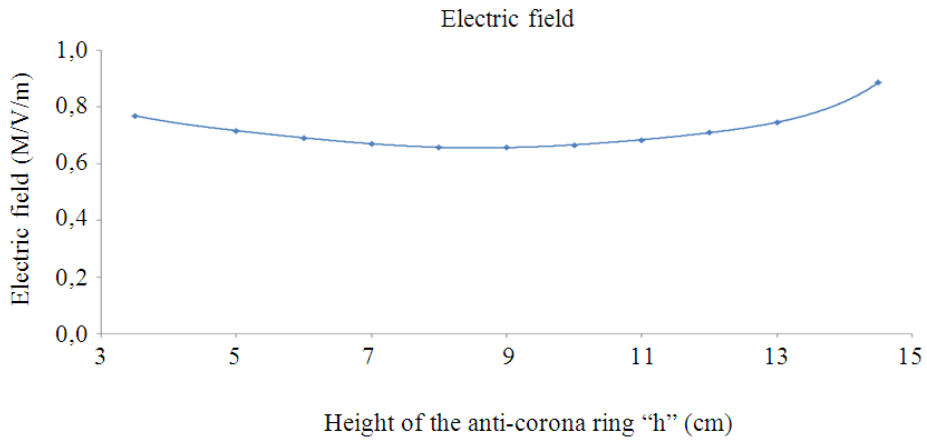
Fig. 12. Graphic showing the electric field for d = 9.0 cm
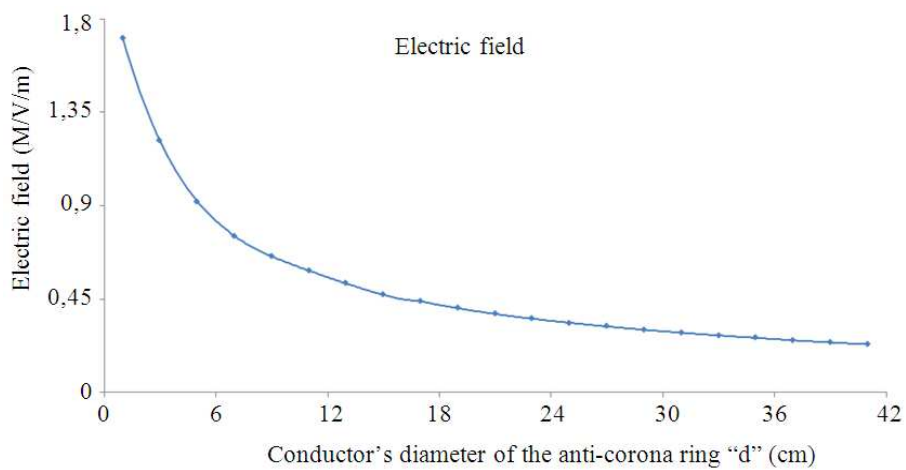
Fig. 13. Graphic showing the variation of the minimum electric field in the isolator

The intersection's value for each simulations set was noted and at the end of these sets of simulations it was possible to obtain the minimum value of the electric field intensity for each value of "d". Thus for each value of "d" in which it was kept fixed it was possible to determine in which height (h) of the anti-corona ring there was a lower electric field intensity. **Figure 12** displays the value of electric field intensity by varying "h" and keeping "d" constant at 9.0 cm.

After determining the minimum point for each value of "d" it was possible to create the graphic of the electric field by varying "d" according to **Fig. 13**.

4. DISCUSSION

Through this study it was possible to investigate the behavior of the electric field in a 500kV voltage class polymeric isolator. The electric field deriving to the isolator's phase terminal can be better equalized using the anti-corona ring, proof of this are in the **Fig. 3 and 4** which shows the electric field in an isolator with the anti-corona ring and without the anti-corona ring, in which it is possible to observe that the peak of the electric field intensity decays when the anti-corona ring is inserted in contrast to a second point of the electric field intensity appears due to the presence of the anti-corona ring. As this electric field event appears several times per second it was considered that the minimum electric field would be when the 1st and 2nd peaks presented the same value.

5. CONCLUSION

In conclusion, it was possible to perform simulations varying the three dimensions of the anti-corona ring: Height (h), distance of the anti-corona ring conductor (r) and the diameter of the anti-corona ring conductor (d). The simulations were performed varying only one parameter at a time, after the analysis of the simulations results, it was observed the value of electric field in the presence of the anti-corona ring and it was shown that this is related to the height of the anti-corona ring and that the electric field intensity decays by increasing the electric field conductor's diameter, which end up presenting a curve as observed in **Fig. 13**.

The electric field that a polymeric isolator can resist without failure is related to the materials used for manufacturing it. As an example, the silicone rubber resistance to tracking, so for the sizing of the anti-corona ring these values must be taken into consideration.

5. REFERENCES

Cardoso, 1995. Introduction to the finite element method for electrical engineers (in portuguese). São Paulo, Brasil, p: 3-33.

ERC, 2012a. National electric energy consumption per class (in portuguese). Energy Research Company (ERC).

ERC, 2012b. Electric energy demand-10 years. Energy Research Company (ERC).

ERC, 2012c. Decennial energy expansion plan-2020. Energy Research Company (ERC).

Halliday, D., R. Resnick and J. Walker, 2010. Fundamentals of Physics. 9th Edn., John Wiley and Sons, Hoboken, NJ., ISBN-10: 0470469110, pp: 1136.

Jardini, J.A., G. Nicola and E. Watanabe, 2011. Alternativas não Convencionais para Transmissão de Energia Elétrica em Longas Distâncias. Brasília.

Leao, R.M., 2008. Radio interference from high voltage power lines. 1st Edn., Porto Alegre, ISBN: 8574307793, pp: 146.

Mello, 2007. Evaluation trials of radio interference and corona visual in isolator chains.

Silva, 2012a. Interference of the anti-corona ring variation in the distribution of the electric field in isolators of the 500 kV voltage class. Proceedings of the 4th Brazilian Symposium on Electrical Systems (BSES' 2), Goiânia (in portuguese).

Silva, 2012b. Dimensioning the anti-corona ring in polymeric isolators for the 500 kV voltage class through the electric field study. Proceedings of the 6th Workshop Postgraduate and Research of the Centro Paula Souza (in portuguese).